Silicon (2017) 9:31–38
DOI 10.1007/s12633-015-9350-3

ORIGINAL PAPER

Sputtered AZO Thin Films for TCO and Back Reflector Applications in Improving the Efficiency of Thin Film a-Si:H Solar Cells

Arokiyadoss Rayerfrancis[1,2] · P. Balaji Bhargav[1,2] · Nafis Ahmed[1,2] · Sekhar Bhattacharya[1] · Balaji Chandra[1] · Sandip Dhara[3]

Received: 7 May 2015 / Accepted: 17 August 2015 / Published online: 12 September 2015

Abstract We report the properties of Al doped ZnO (AZO) thin films on glass substrates and its effect on the efficiency of amorphous silicon (a-Si:H) solar cells as the back reflector. Oriented AZO thin films were grown using DC magnetron sputtering by varying Ar gas flow rates. The influence of Ar flow rate on the structural, electrical and optical properties of AZO thin films suitable for transparent conducting oxide (TCO) and back reflector applications was investigated. The (a-Si:H) solar cells, with and without AZO back reflector, were fabricated on FTO coated glass substrates using the PECVD technique. The solar cells were tested using a Sun simulator under AM 1.5 condition. Enhancement in current density from 12.46 to 14.24 mA/cm^2 with the AZO back reflector was observed, thereby increasing the efficiency of the solar cell from 6.38 to 7.82 %, respectively.

Keywords AZO · a-Si:H solar cell · Back reflector · Structural · Electrical · Optical properties

✉ P. Balaji Bhargav
balajibhargavp@ssn.edu.in

1 SSN Research Center, SSN College of Engineering, Kalavakkam, Tamilnadu, 603110, India

2 Department of Physics, SSN College of Engineering, Kalavakkam, Tamilnadu, 603110, India

3 Surface and Nanoscience Division, Indira Gandhi Centre for Atomic Research, Kalpakkam, 603102, India

1 Introduction

Improving the efficiency of amorphous silicon (a-Si:H) solar cells by light trapping has been intensively studied in recent years. The path length of the light travel inside the device can be increased by reflecting at the rough surface at the back of the active material, which can enhance the absorption [1]. In the a-Si:H solar cells with $p-i-n$ configuration, the metal oxide based semiconductors are introduced in between the active material and the metal back contact. This reflects the unabsorbed light back into the solar cell and therefore the light trapping can be achieved efficiently [2]. Thin film a-Si:H solar cell requires a wide bandgap transparent conductor as window (or front) electrode for efficient light transmission as well as extraction of photocurrent. These properties are most commonly realized through the use of heavily doped, wide band gap metal oxide semiconductor materials [3]. Presently, the most widely used transparent conducting oxides (TCOs) for front electrode application are In_2O_3, SnO_2 and doped ZnO, which are typically doped using Sn (In_2O_3:Sn, ITO), F (SnO_2:F, FTO) and Al (ZnO:Al) or B (ZnO:B), respectively [4, 5]. Generally, transparent conductors deposited and annealed at high temperature exhibit high transmission and electrical conductivity, and are used as TCO for a-Si:H based solar cells deposited on glass substrates [6–8]. However, in the case of a-Si:H solar cells fabricated on flexible substrates, which employs a substrate configuration, the TCO layer is deposited after the deposition of a-Si:H layers. Normally intrinsic and doped a-Si:H layers are deposited at $200-220°C$ using the PECVD technique [9]. So, the TCO layer that will be deposited on the a-Si:H layers needs to

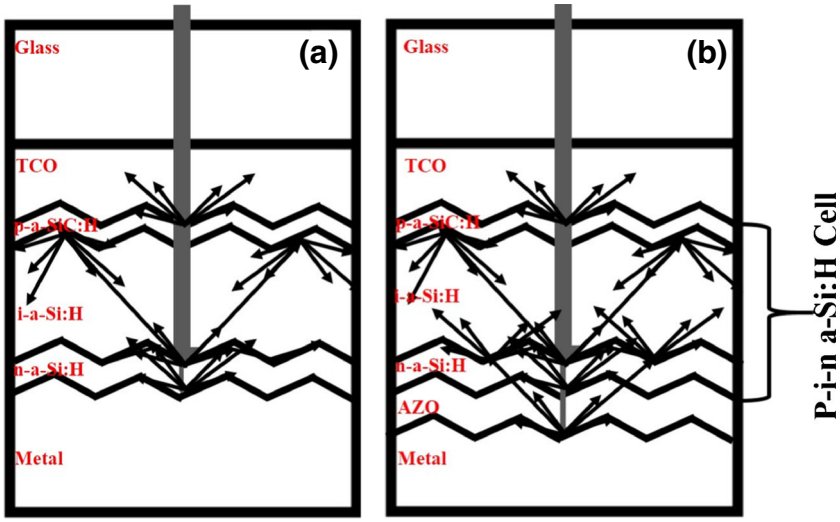

Fig. 1 Schematic of p-i-n a-Si:H solar cell on FTO coated glass substrate (**a**) without back reflector and (**b**) with AZO back reflector

be deposited at relatively lower process temperatures than that of a-Si:H layers. Since, TCO is used as top layer for a-Si:H solar cell in substrate configuration, the selection of the most appropriate material should possess properties like compositional stability during processing [10], environmental stability [5], low toxicity [11, 12] and low production cost. During this decade, numerous investigations have been made on doped ZnO, because of its multifunctional properties, including optical [13], piezoelectric [14], and optoelectronic properties [15]. Doped ZnO films have emerged as an alternative to SnO_2:F and ITO on laboratory scales [16]. Incidentally, doped ZnO films are more resistive to hydrogen plasma than ITO [10]. ZnO films can be conveniently deposited by sputtering or by the low pressure chemical vapor deposition technique [17–19].

In this study, the effect of Ar flow on the structural, optical and electrical characteristics of the AZO thin films, suitable for TCO as well back reflector applications in a-Si:H solar cells is investigated. The role of AZO back reflectors in enhancing the absorption of light was identified by the improved short circuit current density of a-Si:H solar cells.

2 Experiment

Corning glass (Eagle Xg) was used as substrate to study the structural, optical and electrical properties of the AZO thin films. The substrates were cleaned with acetone, isopropyl alcohol and deionized water to remove contaminants from the surface. The AZO films were deposited using a DC magnetron sputtering system. A commercial (ITASCO, South Korea) ceramic target of ZnO (2 wt% Al_2O_3) with 2 inch diameter was used as the sputtering material. The glass substrates were located 7 cm vertically above the target. The sputtering chamber was initially evacuated to $6x10^{-6}$ mbar. A controlled flow of Ar gas was introduced into the chamber with the help of a mass flow controller. Basic parameters like operating pressure (0.01 mbar) and power density (4.4 W/cm^2) were kept constant throughout the process.

Upon the optimization of AZO thin film properties, the film with suitable properties were used in the a-Si:H solar cell for back reflector applications. The a-Si:H solar cells (1cm X 1cm) in $p-i-n$ superstrate structure were fabricated on commercially available fluorinated tin oxide (FTO) glass substrates using plasma enhanced the chemical vapor deposition (PECVD) technique. The amorphous silicon layers were deposited at 220 ^{o}C with 13.56 MHz RF discharge with SiH_4, H_2 for intrinsic a-Si:H, SiH_4, H_2, PH_3 and SiH_4, H_2, CH_4, B_2H_6 for n-a-Si:H and p-a-SiC:H layers respectively. The process pressure of 1000 mTorr and the plasma power of 10 W was maintained throughout the process. The Al metal back contact was deposited by using thermal evaporation technique. Two sets of solar cells with following structure are fabricated and the schematic is shown in Fig 1.

1. Cell 1: Glass/FTO/p-a-SiC:H/i-a-Si:H/n-a-Si:H/Al
2. Cell 2: Glass/FTO/p-a-SiC:H/i-a-Si:H/n-a-Si:H/Al: ZnO/Al

Surface morphology and roughness of the film were studied by using a Veeco Dimension V SPM atomic force microscope (AFM).The crystalline nature of these films was investigated by Seifert Analytical X-Ray diffractometer (XRD) using Cu-K_α radiation with a wavelength of 0.15418 nm. Thickness of the films was measured using DektakXT (Bruker) stylus profilometer with depth resolution of 1 Å max at 6.55 μm range. The optical transmission spectra were measured in the wavelength range from 200 to 1100 nm by using Perkin Elmer lambda 650 UV-VIS-NIR spectrophotometer. FTIR studies were made by using

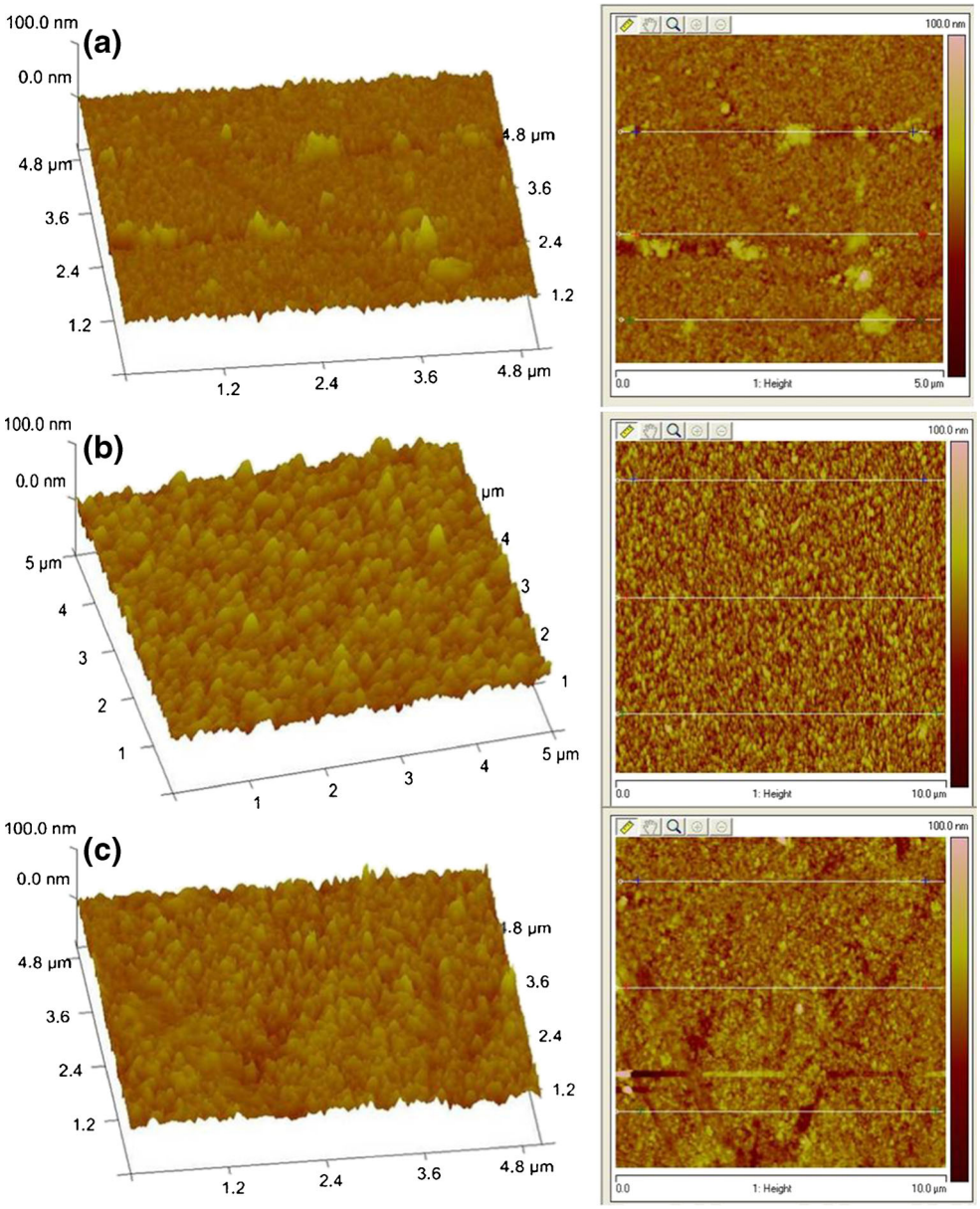

Fig. 2 3D and 2D height profile AFM Image of AZO thin film deposited at different Ar flow rates of (**a**) 40 sccm, (**b**) 30 sccm, and (**c**) 20 sccm

Bruker Alpha T in the wave number range 400 to 4000 cm^{-1} in specular reflection mode. The electrical properties were measured using the Ecopia HMS 5000 Hall measurement technique. The light generated current-density versus the voltage (J-V) characteristics of the fabricated solar cells were measured using solar simulator at AM 1.5 conditions.

3 Results and Discussion

3.1 Surface Morphology

The 3D and 2D height profile images obtained from AFM studies of AZO thin films deposited at different Ar flow rates at 150 °C temperature and 4.4 W/cm^2 power density are shown in Fig. 2. The root mean square roughness of the films deposited at 40, 30 and 20 sccm are 5.6, 8.9 and 8.3 nm, respectively. At 40 sccm of Ar flow rate, a relatively smooth film is observed as sufficiently large Ar gas density inside the chamber reduces the energy of sputtered atoms in the plasma due to internal collisions before reaching the substrate [20]. Not much change in roughness has been observed at 20 and 30 sccm of Ar flow rates. However, for solar cell applications the TCO should have texturing in order to increase the light trapping mechanism by increasing the diffuse transmitted light into the solar cells. According to AFM studies, it is clear that the films deposited at 20 or 30 sccm of Ar flow may be suitable for TCO applications.

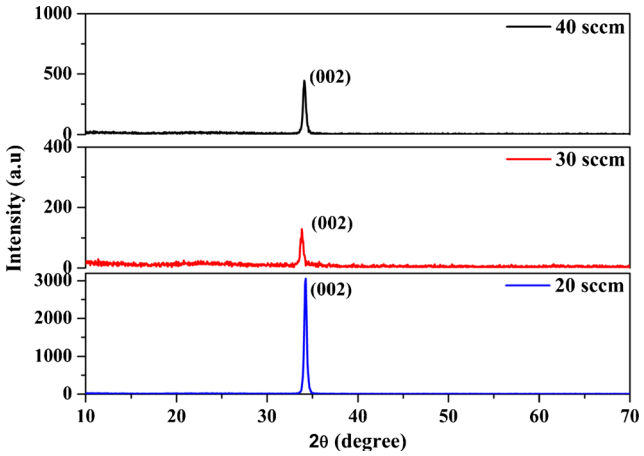

Fig. 3 XRD pattern of AZO thin film deposited at 150°C at different Ar flow rates

3.2 Crystallographic Structural Studies

The structural studies of AZO thin films deposited at different Ar flow rates are reported using XRD analysis. Typical XRD pattern of AZO film grown at different flow rate is shown in Fig. 3. All the films deposited at 150°C with different Ar flow rates, exhibited single *c*-axis oriented peak at 2θ value of 34.14°, 33.85° and 34.24° corresponding to (*hkl*) value of (002) which matches wurtzite phase of ZnO (JCPDS # 36-1451). At this temperature, the deposited films are polycrystalline in nature and the crystallite sizes of the films were calculated by Scherrer formula [21] using the data obtained from XRD. The crystallite sizes in the films are 21.98, 20.50 and 25.61 nm for the films deposited at 40, 30 and 20 sccm, respectively. Increase in the crystallite size of the film was observed from 40 to 20 sccm of Ar flow rate and in between at 30 sccm the crystallite size was decreased. The values were given in Table 1.

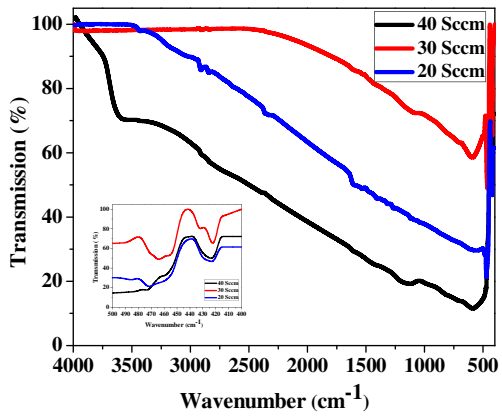

Fig. 4 Spectra of AZO thin film deposited at 150°C at different Ar flow rates

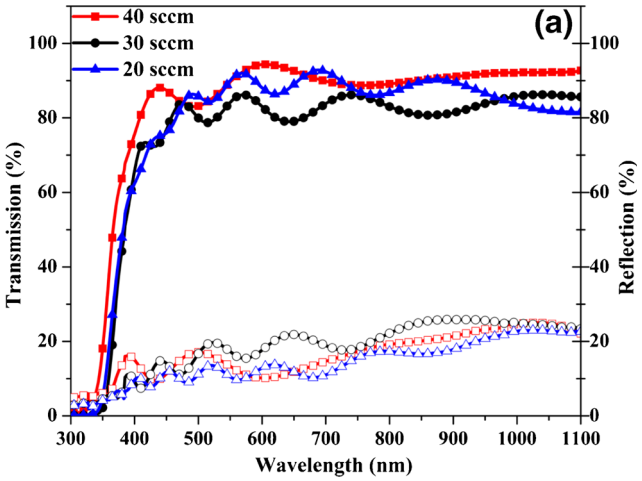

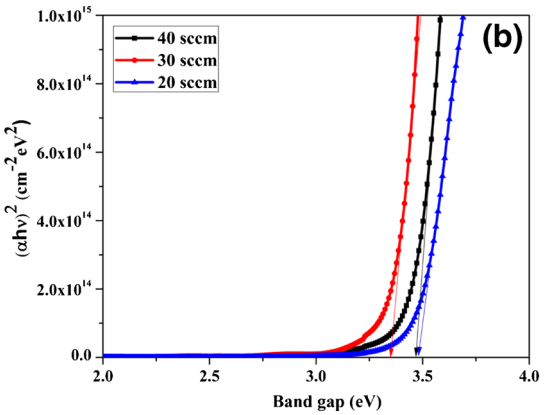

Fig. 5 **a** UV-Vis transmission reflection spectra of AZO thin film deposited at 150°C and (**b**) Tauc's plot for evaluating band gap of AZO thin film deposited at 150 °C at different Ar flow rates

3.3 Chemical Bond Formation

In order to verify the bond formed between Zn and O, the AZO thin films were characterized using Fourier Transformed Infra-Red spectroscopy (FTIR). The spectrum shows (Fig. 4) two peaks at 422 and 471 cm^{-1}, which belong to Zn-O stretching mode of vibration [22]. No other peaks of impurity were observed ensuring chemical purity of the deposited.

3.4 Optical Characterizations

UV-Vis transmission and reflection spectra of AZO thin film deposited at 150°C are shown in the Fig. 5(a). The overall transmission of the films deposited at a deposition temperature of 150 °C and at a power 4.4 W/cm^2 is more than 80 % with a compliment reflection throughout the visible region. These values are very similar to ~85 % transmission of the ITO films reported previously for TCO applications [23, 24]. Generally, active layers in the a-Si:H solar cells absorb light in the wavelength range of 400-800 nm [25]. So the

Table 1 FWHM, grain size, and roughness of AZO thin films

Process Parameters		Peak Position(°)	FWHM (°)	Grain size (nm)	RMS Roughness (nm)
150°C 4.4 W/cm^2	40 sccm	34.14	0.392	21.98	5.6
	30sccm	33.85	0.423	20.50	8.87
	20 sccm	34.24	0.339	25.61	8.3

TCO material also should exhibit better transmission in the above mentioned wavelength range, in order to allow more light entering into the solar cell, to enhance the efficiency of the solar cell. From the transmission data, the band gap of AZO films was calculated using Tauc's plot (Fig. 5(b)) following Eq. 1.

$$(\alpha h\nu)^2 = A(h\nu - E_g) \tag{1}$$

where α is the absorption coefficient, h is the Planck's constant and ν is the frequency of radiation. The band gaps (E_g) of the AZO film deposited at 40, 30 and 20 sccm of Ar flow rate are 3.46, 3.35 and 3.48 eV, respectively. According to Burstein-Moss (B-M) effect, the band gap of the doped semiconductors will increase with the increase of carrier concentration due to the Fermi level shift [26]. In the present investigations, the calculated band gap values are following the equivalent trend with the carrier concentration values measured using Hall Effect measurements given in Table 2.

Table 2 The values of λ, T_M, T_m, and Refractive Index (n) for the AZO films deposited at different flow rates.

λ (nm)	T_M	T_m	Refractive index of glass (s)	N	Refractive Index (n)
40 sccm					
437	0.883	0.759	1.55	2.274813	1.9849
495	0.932	0.83	1.55	2.11001	1.881931
606	0.944	0.872	1.55	1.972398	1.786665
780	0.944	0.889	1.55	1.904416	1.735194
					1.847173
30 sccm					
475	0.84	0.768	1.55	2.047232	1.839739
516	0.857	0.786	1.55	2.028001	1.826412
572	0.862	0.792	1.55	2.019104	1.820177
645	0.864	0.788	1.55	2.047297	1.839784
740	0.862	0.796	1.55	1.999435	1.806229
					1.826468
20 sccm					
520	0.894	0.843	1.55	1.911031	1.740362
568	0.92	0.858	1.55	1.944738	1.766143
624	0.929	0.865	1.55	1.948144	1.768699
689	0.927	0.866	1.55	1.936806	1.760156
775	0.918	0.862	1.55	1.920631	1.747797
					1.756632

3.5 Refractive Indices Using Swanepoel's Calculations

The refractive indices (n) of the film were calculated from the transmission spectra, using Swanepoel's calculations. The property that thin films absorb light in the ultraviolet, visible and near infrared regions can be significantly utilized due to their uses in photothermal and photovoltaic conversion of solar radiation. Swanepoel proposed a straight forward idea that the n and α of the thin film can be calculated using the transmission spectrum alone [30, 31]. The series of transmission maximum (T_M) and transmission minimum (T_m) were observed as a function of wavelength (λ) in the transmission spectra of the film using envelope method (Fig. 6). The refractive index of the film is calculated by

$$n(\lambda) = [N + (N^2 - s^2)^{1/2}]^{1/2} \tag{2}$$

where N is defined as,

$$N = 2s\frac{T_M - T_m}{T_M T_m} + \frac{s^2 + 1}{2} \tag{3}$$

and s is the refractive index of the glass substrate ($s = 1.5$).

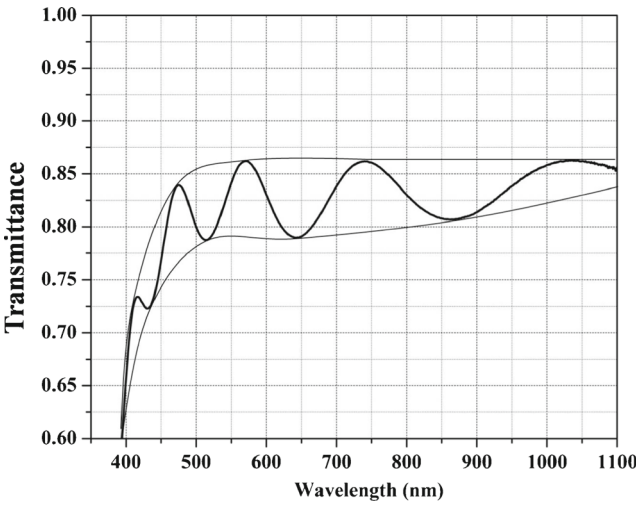

Fig. 6 Transmission spectra of AZO thin film deposited at 150°C / 4.4W/cm^2 / 30 sccm on corning (EagleXg) glass substrate from the experimental results

Table 3 Deposition rate, carrier concentration, sheet resistance, resistivity, and mobility of the AZO thin films

S. No.	Sample	Dep Rate nm/min	Carrier Concentration (cm^{-3})	Sheet Resistance (Ω/Square)	Resistivity (Ω-cm)	Mobility (cm^2/V-s)
1	20 sccm	3.33	$3.08x10^{20}$	22	$1.23x10^{-3}$	17.0
2	30 sccm	1.66	$2.04x10^{20}$	52	$1.49x10^{-3}$	25.6
3	40 sccm	1.33	$2.31x10^{20}$	168	$2.63x10^{-3}$	12.4

The values of λ, T_M and T_m for the AZO films deposited at different flow rate are tabulated in Table 3 and from the Swanepoel's calculations the refractive indices are found to be 1.847, 1.826 and 1.756 for flow rates in the descending order. In order to reduce the optical losses of a-Si:H solar cells, the refractive index of the TCO material should be in between 1.8-2.0 as the refractive indices of a-Si:H and air are ∼3.8 and 1, respectively. Thus the measured values are in the desired range suitable for TCO applications.

3.6 Thickness and Electrical Characterizations

Thicknesses of the AZO thin films were measured using stylus profilometer. The results indicate an increase in deposition rate with decreasing Ar flow rate. The thickness of the films for different flow rates, carrier concentration, sheet resistance, resistivity, conductivity and mobility of the films were obtained from the Hall measurement technique and the values are tabulated in Table 2. The resistivities of the films were $2.63x10^{-3}$, $1.49x10^{-3}$ and $1.23x10^{-3}$Ω-cm for the Ar flow rates of 40, 30 and 20 sccm, respectively. Figure 7 shows the trend obtained for the electrical properties of the AZO thin film with the change in the process parameters. The carrier concentration and the corresponding mobility of the film at 40 sccm were $2.31x10^{20}$ $cm^{-3}$and 12.4 cm^2/V-s, respectively. A maximum value of carrier concentration of $3.08x10^{20}$ cm^{-3} and mobility of 17 cm^2/V-s are observed at Ar flow rate of 20 sccm. But the film deposited at 30 sccm shows a high mobility of 25.6 cm^2/V-s, since the carrier concentration of the film is decreased to $2.04x10^{20}cm^{-3}$. This may be due to decrease in the crystallite size. Generally, the mobility increases with the decreasing carrier concentration and *vice versa* with increasing carrier concentration (˜10^{20} cm^{-3}) due to scattering behavior of electrons [27]. The results obtained in the present investigations are compared with the previous work on the prominent TCO material of ITO [28, 29]. The obtained results of AZO, having enhanced electrical and optical properties, are comparable to that of ITO films which are annealed at high temperatures above 300°C.

4 Back Reflector in a-Si:H Solar Cells

Hydrogenated amorphous solar cells in $p-i-n$ configuration were fabricated on textured FTO coated glass substrates. p-a-SiC:H layer of 18nm, i-a-Si:H layer of 310 nm and n-a-Si:H layer of 30 nm thickness were deposited using PECVD at 220°C using the process gases mentioned in the experimental section. Prior to the fabrication of solar cells, intrinsic and doped a-Si:H layers were optimized by changing the gas flow ratios. The dark and photo conductivity of i-a-Si:H was optimized to the order of 10^{-9} and

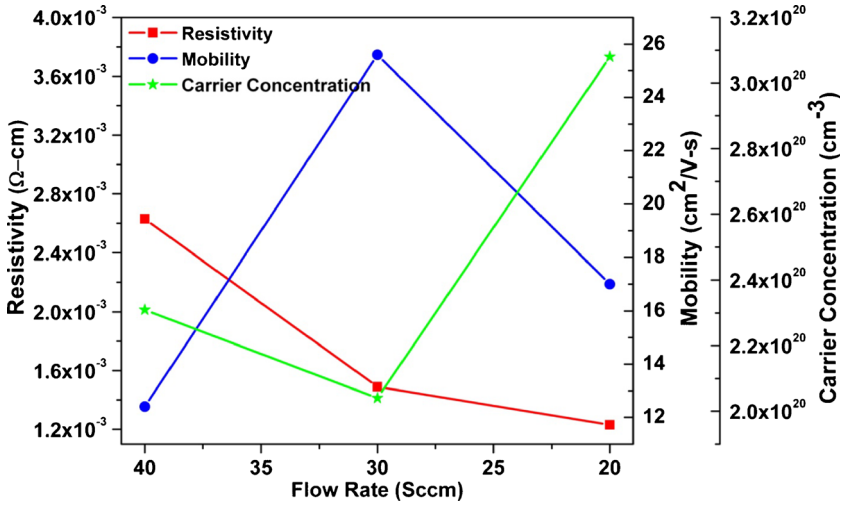

Fig. 7 Resistivity, mobility and carrier concentration of AZO thin film deposited at 150 °C at different Ar flow rates

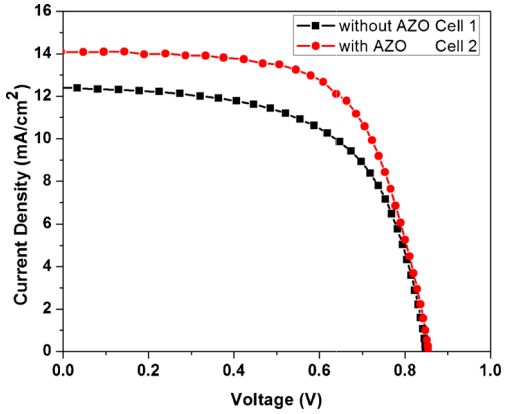

Fig. 8 I-V Characteristics of a-Si:H solar cells with and without AZO back reflector

10^{-5} S/cm. The obtained gain was 10^4. No photo gain was observed in the doped a-Si:H layers. Transmission spectra for the doped and intrinsic a-Si:H layers were recorded in the range of 300-1000 nm using UV/VIS –NIR spectrometer, and the measured band gap values for p-a-SiC:H, i-a-Si:H and n-a-Si:H were 1.85, 1.76 and 1.75 eV respectively. Solar cells were fabricated without AZO and with 90 nm of AZO layer, optimized at 30 sccm of Ar flow in between *n*-a-Si:H and Al metal layer. I-V curves of solar cells with and without back reflector layer were shown in Fig. 8. Solar cell parameters are listed in Table 4. The effect of back reflector AZO is clearly visible by enhancing the current density from 12.46 to 14.24 mA/cm^2, thereby increasing the efficiency from 6.38 to 7.82 %, respectively. The role of back reflector is to increase the back reflection of unabsorbed light again into the solar cells, thereby increasing the light absorption mechanism in the active layers of the solar cell. This will increase the photo generated carrier density, which in turn will affect the generated photo current density [32]. The incorporation of Al:ZnO layer in between, n-a-Si:H and Al back contact, not only improves the light trapping mechanism, but also reduces the inter diffusion of Al layer into the *n*-a-Si:H layer. In addition to light scattering and diffraction upon interaction of light at the metal back contact, an enhanced plasmonic absorption takes place at the rough metal surface. Thereby introducing a back reflector reduces the optical absorption at the metal surface [33].

Table 4 A-Si:H solar cell parameters

Parameters	Without back reflector	With back reflector AZO
V_{oc}(V)	0.849	0.854
J_{sc}(mA/cm^2)	12.46	14.24
FF	0.603	0.643
Efficiency (%)	6.38	7.82

5 Conclusion

Owing to the inherent advantages of AZO compared to its conventional counterpart ITO, it is imperative that it should be optimized for photovoltaic applications. A highly conductive AZO layers were optimized for TCO and back reflector applications in a-Si:H solar cells with DC magnetron sputtering technique. AZO thin films were deposited at a plasma power density of 4.4 W.cm^{-2}, process temperature of 150^{o}C and Ar gas flow rate of 20, 30, and 40 sccm. The film with 30 sccm of Ar flow rate showed the desired roughness, good transmission with the high mobility and low resistivity, making it suitable candidate for TCO and back reflector application in amorphous silicon solar cell. The achieved transmission and resistivity values were ˜85 % and $10^{-3}\Omega$-cm, respectively, as compared to ˜85 % and $10^{-4}\Omega$-cm of ITO grown at ˜300^{o}C. The a-Si:H solar cells in $p-i-n$ configuration were fabricated on FTO coated glass substrates. The effect of back reflector AZO is clearly visible by enhancing the current density from 12.46 to 14.24 mA/cm^2, thereby increasing the efficiency from 6.38 to 7.82 %, respectively.

Acknowledgments The authors sincerely thank UGC-DAE-CSR, India for providing financial support to carry out this work.

References

1. Poortmans J, Arkhipov V (2006) Thin film solar cells fabrication, characterization and applications. Wiley, Chichester
2. Banjeree A, Guha S (1991) Study of back reflectors for amorphous silicon alloy solar cell application. J Appl Phys 69:1030–1035
3. Ogale SB, Venkatesan TV, Blamire MG (2013) Functional metal oxides: new science and novel applications. Wiley-VCH Verlag GmbH & Co. KGaA
4. Chopra KL, Major S, Pandya DK (1983) Transparent conductors - A status review. Thin Solid Films 102:1–46
5. Minami T (2005) Transparent conducting oxide semiconductors for transparent electrodes. Semicond Sci Tech 20:S35–S44
6. Durukan IK, Özen Y, Kizilkaya K, Öztürk MK, Memmedli T, Özçelik S (2013) Effects of annealing and deposition temperature on the structural and optical properties of AZO thin films. J Mater Sci Mater El 24:142–147
7. Fang GJ, Li DJ, Yao BL (2002) Effect of vacuum annealing on the properties of transparent conductive AZO thin films prepared by DC magnetron sputtering. Phys Status Solidi A 193:139–152
8. Sathiaraj (2008) Effect of annealing on the structural, optical and electrical properties of ITO films by RF Sputtering under low vacuum level. Microelectr J 39:1444–1451
9. Shah AV, Schade H, Vanecek M, Meier J, Vallat-Sauvain E, Wyrsch N, Kroll U, Droz C, Bailat J (2004) Thin-film silicon solar cell technology. Prog Photovolt Res Appl 12:113–142
10. Minami T, Sato H, Nanto H, Takata S (1989) Heat treatment in Hydrogen gas and plasma for transparent conducting oxide films such as ZnO, SnO_2 and Indium tin oxide. Thin Solid Films 176:277–282

11. Lison D, Laloy J, Corazzari I, Muller J, Rabolli V, Panin N, Huaux F, Fenoglio I, Fubini B (2008) Sintered Indium-Tin-Oxide (ITO) particles: a new pneumotoxic entity. Toxicol Sci 108:472–481
12. Nagono K, Nishizawa T, Umeda Y, Kasai T, Noguchi T, Goroh K, Ikawa N, Eitaki Y, Kawasumi Y, Yamauchi T, Arito H, Fukushima S (2011) Inhalation carcinogenicity and chronic toxicity of indium-tin oxide in rats and mice. J Occup Health 53:175–187
13. Li F, Wang L, Dai J, Pu Y, Fang W, Jiang F (2007) Photoluminescence observations of hydrogen incorporation and out diffusion in ZnO thin films. J Lumin 124:162–166
14. Riaz M, Song J, Nur O, Wang ZL, Willander M (2011) Study of the piezoelectric power generation of ZnO nanowire arrays grown by different methods. Adv Funct Mater 21:628–633
15. Oh BY, Jeong MC, Moon TH, Lee W, Myoung JM, Hwang JY, Seo DS (2006) Transparent conductive Al-doped ZnO films for liquid crystal displays. J Appl Phys 99:124505
16. Ellmer K, Klein A, Rech B (2008) Transparent conductive zinc oxide: basics and applications in thin film solar cells. Springer Science & Business Media
17. Böttler W, Smirnov V, Lambertz A, Hüpkes J, Finger F (2010) Window layer development for microcrystalline silicon solar cells in n-i-p configuration. Phys Status Solidi C 7: 1069–1072
18. Kluth O, Rech B, Houben L, Wieder S, Èpe GS, Beneking C, Wagner H, LoÈf A, Schock HW (1999) Texture etched ZnO:Al coated glass substrates for silicon based thin film solar cells. Thin Solid Films 351:247–253
19. Cho S (2009) Effects of growth temperature on the properties of ZnO thin films grown by radio-frequency. Magnetron Sputtering Trans Electr Electron Mater 10:185
20. Wu HW, Chu CH, Chen YF, Chen YW, Tsai WH, Huang SH, Chen GS (2013) Study of AZO Thin Films Under Different Ar Flow and Sputtering Power by RF Magnetron Sputtering Proceedings of the International Multi Conference of Engineers and Computer Scientists Vol II IMECS
21. Birks LS, Friedman H (1946) Particle size determination from X-Ray line broadening. J Appl Phys 17:687
22. Kim DS, Part JH, Lee SJ, Ahn KJ, Lee MS, Ham MH, Lee W, Myong JM (2013) Effects of Oxygen Concentration on the properties of Al-doped ZnO Transparent Conductive Films Deposited by Pulsed DC Magnetron Sputtering. Mater Sci Semicond Process 16:997–1001
23. Keum MJ, Han JG (2008) Preparation of ITO thin film by using DC magnetron sputtering. J Korean Phys Soc 53:1580–1583
24. Ali MKM, Ibrahim K, Hamad OS, Elisa MH, Faraj MG, Azhari F (2011) Deposited indium tin oxide (ITO) thin films by DC-magnetron sputtering on polyeleylene terephthalate substrate (PET) Rom. J Phys 56:730–741
25. Solanki CS (2009) Solar photovoltaics fundamentals technologies and applications (PHI Learning Private Limited, Delhi)
26. Kamat PV, Dimitrievic NM, Nozik AJ (1989) Dynamic Burstein-moss shift in semiconductor colloids. J Phys Chem 93:2873–2875
27. Leenheer AJ, Perkins JD, Van Hest MFAM, Berry JJ, O'Hayre RP, Ginley DS (2008) General mobility and carrier concentration relationship in transparent amorphous indium zinc oxide films. Phys Rev B 77(1–5):115–215
28. Rottmannt M, Heckner KH (1995) Electrical and structural properties of indium tin oxide films deposited by reactive DC sputtering. J Phys D Appl Phys 28:1448–1453
29. Kerkache L, Layadi A, Dogheche E, Remiens D (2006) Physical properties of RF sputtered ITO thin films and annealing effect. J Phys D Appl Phys 39:184–189
30. Swanepoel R (1983) Determination of the thickness and optical constants of amorphous silicon. J Phys E Sci Instrum 16:1214–1222
31. Ahmed N, Singh CB, Bhattacharya S, Dhara S, Bhargav PB (2013) Optical and structural properties of ammonia-free amorphous silicon nitride thin films for photovoltaic applications. Spectrosc Lett 46:493–498
32. Cho JS, Baek S, Park SH, Park JH, Yoo J, Yoon KH (2012) Effect of nanotextured back reflectors on light trapping in flexible silicon thin-film solar cells. Sol Energy Mater Sol Cells 102:50–57
33. Palanchoke U, Jovanov V, Kurz H, Obermeyer P, Stiebig H, Knipp D (2012) Plasmonic effects in amorphous silicon thin film solar cells with metal back contacts. Optic Express 20:6340–6347